Wideband Self-Interference Channel Modelling for an On-Frequency Repeater

Sathya N. Venkatasubramanian[1], Leo Laughlin[2], Katsuyuki Haneda[1] and Mark A. Beach[2]
[1]Dept. of Radio Science and Engineering, Aalto University, School of Electrical Engineering, Espoo, Finland.
[2]Dept. of Electrical and Electronic Engineering, University of Bristol, Bristol, United Kingdom.

***Abstract*—In-band full-duplex relaying has been of recent interest as it can potentially double spectral efficiency and decrease latency, thus improving throughput to the end user. The bottleneck in enabling full-duplex operation is the self-interference (SI) due to the relay's own transmission, which must be mitigated at the antenna, radio frequency and digital domains. In the case of compact back-to-back relays which are proposed for outdoor-to-indoor relaying, the SI comprises direct coupling and multipath components. This paper models the SI channel across 300 MHz bandwidth at 2.6 GHz in two indoor environments with a back-to-back relay antenna. The power delay profile of the SI channel is modelled as a single decaying exponential function with specular components represented by delta functions. The fading characteristics of each tap are modelled by a normal distribution based on the measurements. The proposed model can be used to generate a tapped-delay model of the SI channel between compact back-to-back antennas for use in link-level simulations and hardware in the loop emulation.**

***Index Terms*—antenna, propagation, full-duplex, relays.**

I. Introduction

In-band full-duplex (IBFD) communications is a promising technique for future wireless systems that increases the throughput to the end user [1], [2]. Relays are expected to be among the first devices to deploy IBFD, where it can result in improved spectral efficiency and decreased latency. The main bottleneck to IBFD operation is the self-interference (SI) caused at the relay receiver by its own transmission. Many techniques have been proposed in order to mitigate the SI such that it can be avoided or cancelled at the antenna, radio frequency and digital domains.

One of the possible scenarios envisaged for relay deployment is outdoor-to-indoor coverage extension, where the relay is deployed near a window with the receive (Rx) antenna(s) facing the base station and transmit (Tx) antenna(s) covering the indoor area in the downlink case. The SI in this case is caused not only by the direct coupling between the closely spaced Tx and Rx antennas, but also due to multipath propagation between them, e.g. signals reflected from the close-by windows and other objects, and previous work has shown that this multipath can affect the Tx-Rx isolation [3]–[5].

The research work leading to these results was funded by the Academy of Finland, under the project In-band Full-Duplex MIMO Transmission: A Breakthrough to High-Speed Low-Latency Mobile Networks (decision number 259915), by the Aalto ELEC Doctoral School, and the UK EPSRC through the CDT in Communications (EP/I028153/1).

The design of SI cancellation methods generally involves applying an SI channel model to the transmit signal in order to generate the cancellation signal. The effectiveness of a particular cancellation method depends on the accuracy of the channel model, and various SI channel models have been reported in the literature. In [6], [7], narrowband channel models are employed, applying a frequency invariant amplitude and phase shift to generate the cancellation signal, effectively modelling only the direct coupling. The system described in [6] achieves 37 dB of cancellation over a relatively narrow 200 kHz bandwidth using the frequency invariant channel model, however the isolation of systems such as this deteriorates significantly for wider bandwidths. This demonstrates that, to achieve wideband isolation, it is necessary to model the frequency selective characteristics which arise from multipath propagation. In [4], it is shown that the number of taps required in a time domain SI canceller increases as the K-factor of the SI channel reduces, and thus, as would be expected, an SI channel with more pronounced multipath characteristics requires a model with more taps. In [8], [9] the SI channel is modelled in the discrete frequency domain, a model commonly applied for channel equalisation in orthogonal frequency division multiplexing systems, and it is shown that a 15 kHz subcarrier spacing, as employed in LTE, can model the SI channel with sufficient accuracy. Previous work on relay antenna SI channels [5], [10] has investigated the mean isolation level averaged over wide bandwidth at 2.6 GHz for indoor relays, but does not discuss the wideband characteristics of the SI channel. Thus, there is a need to develop wideband SI channel model which includes the fading characteristics of the channel.

In this contribution, the wideband SI channel is analysed for compact on-frequency repeaters in two indoor scenarios. The power delay profile (PDP) of the SI channel is characterized over a bandwidth of 300 MHz. The PDP is modelled as an exponentially decaying function, while the small-scale fading characteristics of each tap are described with normally distributed K-factors. The channel model developed in this paper can be used for link level simulations in order to generate SI channels as well as to develop decoupling techniques for improving the wideband antenna isolation [11] of compact on-frequency relays in indoor multipath environments.

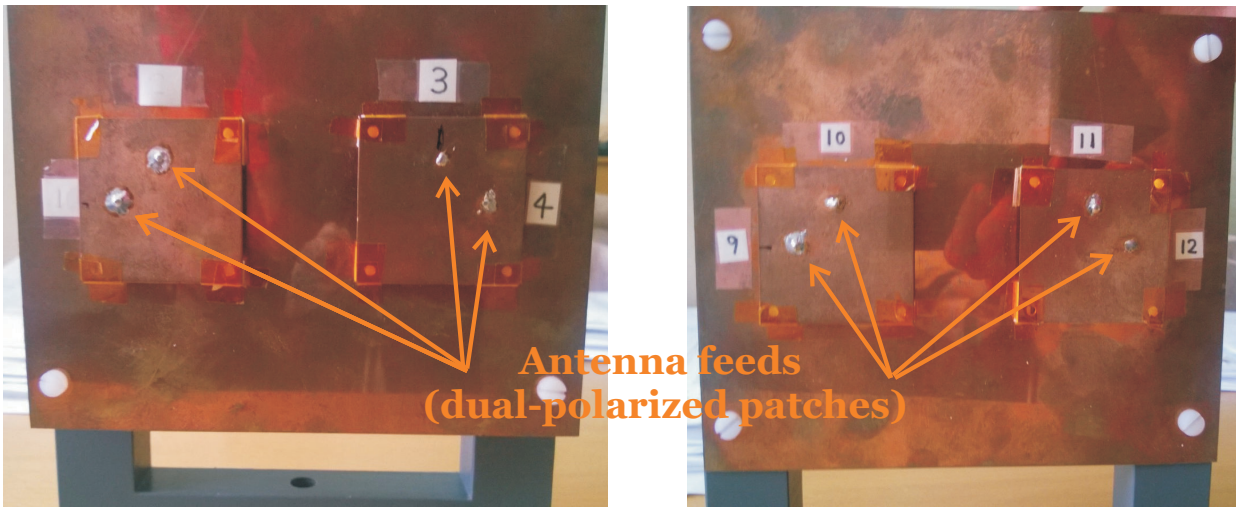

Fig. 1. Image of the antenna, both front and rear sides. Ports 1-4 and 9-12 were facing the room and windows respectively, representing the Tx and Rx for downlink scenario.

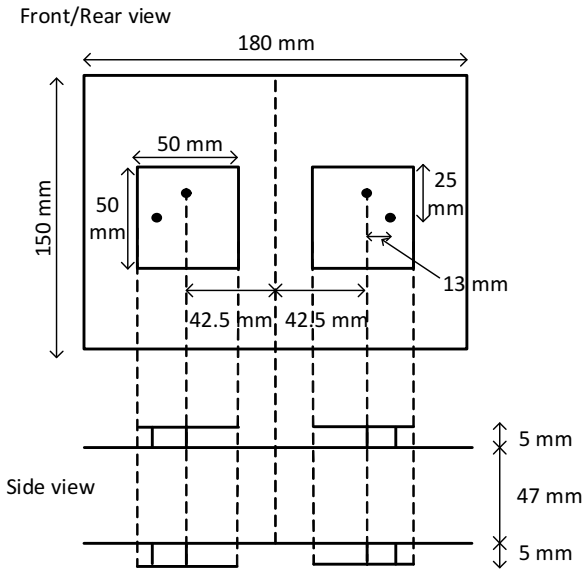

Fig. 2. Schematic representation of the relay antenna. Each side of the relay comprises two dual-polarized patch antennas operating at 2.6 GHz. The two ground planes are fixed using nylon screws.

II. Antenna Configuration and Measurement Setup

For the SI channel measurements from which the model is derived, a compact relay device consisting of back-to-back patch antennas was chosen. The dimension of the device is $180 \times 150 \times 57\text{mm}^3$. This antenna is similar to that previously reported in [5], however the presently reported antenna has identically polarized elements on different sides of the relay, whereas the device in [5] used elements with slanted polarizations. Fig. 1 shows the image of the antennas on both sides with feeds locations indicated. The rear side of the antenna has a similar configuration with identical feed locations, i.e., the feed on the other side of the relay is exactly behind the feed on the front side. Fig. 2 shows the schematic diagram of the antenna. The relay comprises two ground planes spaced by 47 mm using nylon screws. The relay box is open in the sides, i.e. the two ground planes are not connected (as would be the case in a closed metallic box configuration) such that the feed cables could be attached easily. Two dual-polarized patch antennas are located 5 mm above each ground plane, facing outward as shown in the side view in Fig. 2. Short cables are connected at each feed in order to measure the scattering parameters between each antenna port combination. The effect of the short cables was removed when analysing the channel data and hence, the reference plane is at the connector input at each feed location. As there are two dual-polarized patch antennas on either side of the relay, it corresponds to four ports on either side. We assume that the four ports on one side serve for Tx, and another four on the other side for Rx. If we consider the coupling channels between the Tx and Rx ports, then there are 16 port combinations (4×4), resulting in 16 coupling channels. Of these 16 channels, eight are between Tx and Rx antenna ports with the same polarization, and the other eight are between antenna ports with orthogonal polarizations.

The antenna feeds have better than -6 dB input matching over varying bandwidths between 257 and 300 MHz around 2.6 GHz depending upon the feed. Hence the SI channel measurements were performed across 300 MHz bandwidth around 2.6 GHz, i.e. between 2.45 to 2.75 GHz. The mutual coupling between the antenna ports in the anechoic chamber, which refers to the direct component in the SI channel varies between -40 to -80 dB for the co-polarized and cross-polarized port combinations. The SI channels were measured using an Agilent N5242 PNA-X Vector Network Analyser (VNA) with intermediate Frequency (IF) bandwidth of 100 kHz and with frequency sweep points at 500 kHz intervals across the 300 MHz measurement bandwidth.

The antenna was mounted on a tripod and the SI was measured for all the antenna port combinations on either side of the relay, and in various locations near the window in two indoor environments: a reception room and a coffee room.

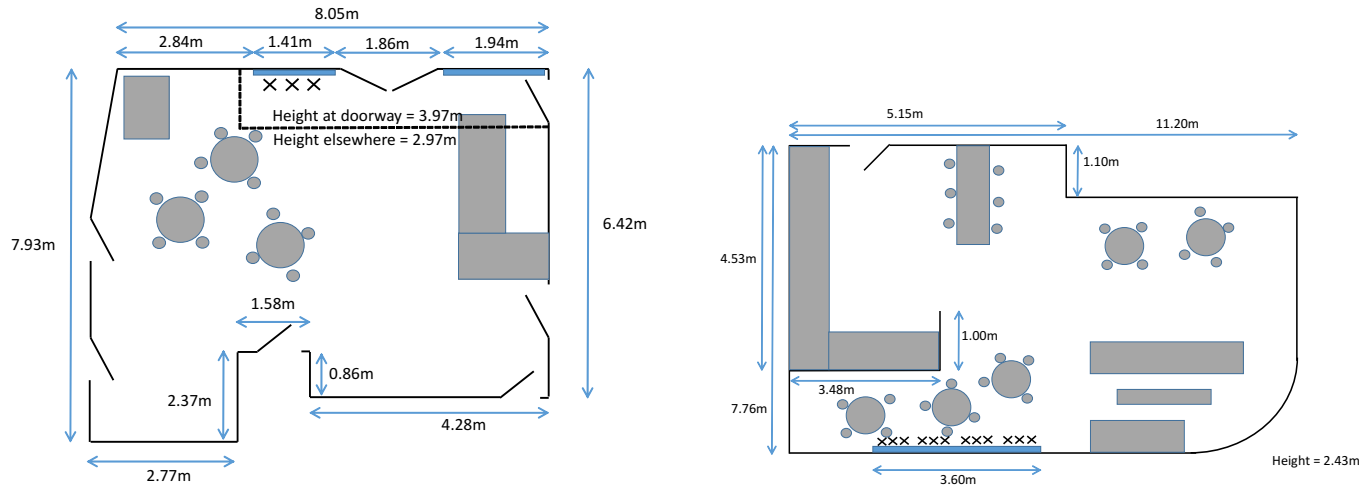

(a) (b)

Fig. 3. Layout of the measurement sites, (a) Reception and (b) Coffee Rooms. The dark shaded portion indicates the windows in the room. The locations marked with a cross indicate the measured locations. At each location, the SI channels were measured with multiple relay heights.

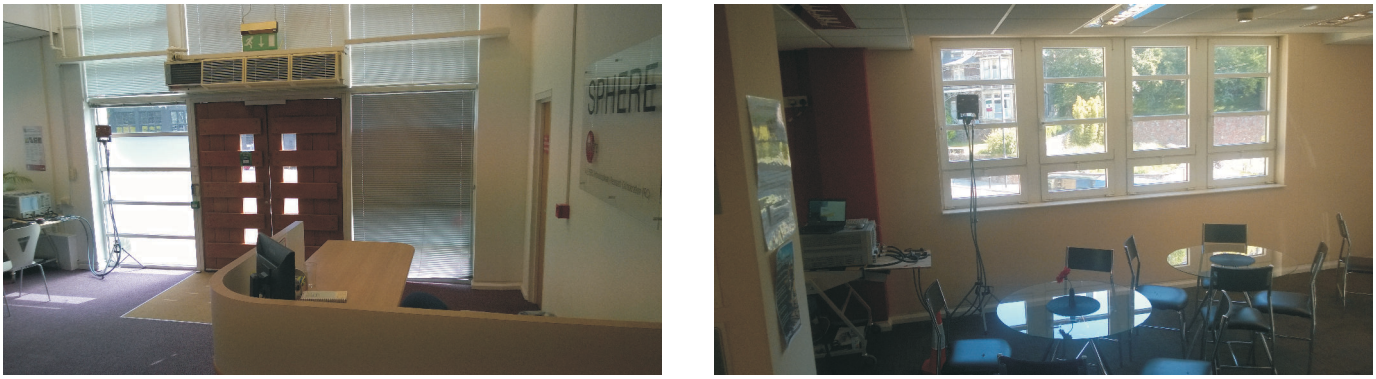

(a) (b)

Fig. 4. Image of measurement setup with antenna mounted on a tripod in (a) Reception room and (b) Coffee Room. The relay is located adjacent to the window.

Layout and image of the two rooms are shown in Figs. 3 and 4, respectively. The two rooms were selected for measurement convenience as well as human activity in order to characterize the time varying SI channel. The window of the reception room is at ground level and overlooks a busy main road while the coffee room is one level above the ground level overlooking a road which has less traffic compared to the reception location. In the coffee room, measurements were performed at 12 locations near the window, and at each of these locations measurements were taken at 6 antenna heights. The antenna heights were at 2 cm intervals between 180 cm and 190 cm. In the Reception room 3 locations were measured using 11 antenna heights at each of these locations. In this case the antenna heights were at 2 cm intervals between 170 cm and 190 cm. The antennas were placed as close to the windows as possible with the tripod mount. The dark blue shaded portions in Fig. 3 indicate the windows in the room and the measurement locations are indicated with a cross near the windows. An SI channel of single Tx-Rx port combination at given location and height was measured at a given time for approx. 30 s, corresponding to 501 continuous frequency sweeps in the VNA. The remaining ports were terminated with 50Ω impedance. The input matching of the antenna feeds were also measured to analyse their changes when deploying antennas close to the window, however the variation in the matching is beyond the scope of this paper.

III. Results and Discussion

In this section, the delay domain characteristics of the SI channel are modelled from power delay profiles (PDPs) of the measured channels; number of taps and the fading distribution for each tap is provided.

A. Power delay profile

The channel transfer function matrix is measured between the feed connectors of the antennas, and consists of 501

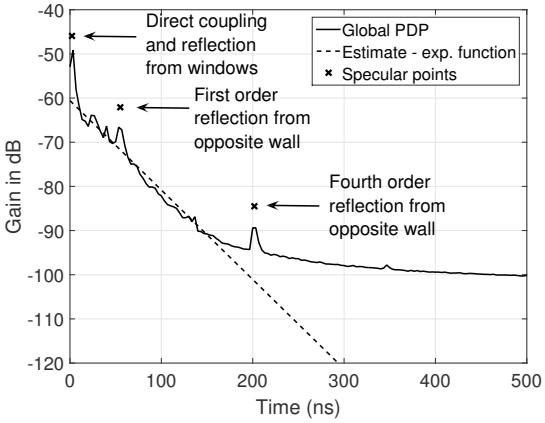

Fig. 5. Global PDP of the SI channel. Dashed line shows the estimated exponentially decaying diffuse spectrum and the specular components indicated by crosses.

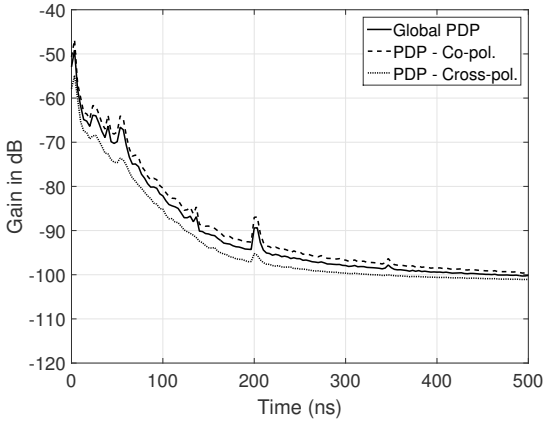

Fig. 6. Global and polarisation-specific PDPs; The co-/cross-polarized PDPs are from the same/differently polarized antenna ports on either side of the relay.

frequency sweep points for each port combination, measured at various locations and heights for both the rooms. Each measured channel transfer function is transformed into the channel impulse response (CIR) using the discrete inverse Fourier Transform. Since the channel was sampled every 500 kHz, the duration of the CIR is 2μs which is sufficient to observe the long-delayed multipath components without aliasing. The 300 MHz measurement bandwidth corresponds to a sampling period of 3.33 ns, which translates to 1 m propagation distance. The PDP for each Tx-Rx port combination is derived as the ensemble average of the powers of 501 CIRs obtained from varying antenna height and locations to provide a single SI channel model for the measured scenario. The PDP of the SI channel for each room is then obtained as the mean of the PDP across each antenna port combination. Since the PDPs of the two rooms were similar, they were incoherently averaged to yield a *global* PDP of the SI channel. In addition to the global PDP, polarization specific PDPs are also computed. These represent the average PDPs taken across the cross polar and co-polar channels separately. Fig. 5 shows the global PDP and their model, consisting of exponentially decaying power spectrum with specular components that appear as peaks at certain delays. The model defined in the linear scale is described as

$$PDP(\tau) = \alpha \left\{ \sum_{n=1}^{N} P_n \delta(\tau - \tau_n) + P_{\text{dif}} \exp\left(-\frac{\tau([\text{ns}])}{\beta} \right) \right\}, \tag{1}$$

where α denotes the dependence of the SI level on Tx and Rx antenna polarizations as

$$\alpha = \begin{cases} 0\,\text{dB} & \text{for global PDP} \\ 2.64\,\text{dB} & \text{for co-pol PDP} \\ -5.08\,\text{dB} & \text{for cross-pol PDP} \end{cases}, \tag{2}$$

$P_{\text{dif}} = 8.75 \times 10^{-7}$ is the peak power of the exponentially decaying power spectrum observed at $\tau = 0$ ns and $\beta = 21.5$.

The power and delay of the specular components are given in Table I. The specular peaks are detected if they are greater than the diffuse component or the noise level by 3 dB; in our measurement, $N = 3$. If a specular peak is detected across two adjacent bins, then the corresponding peak power and delay of the peak are estimated by comparing the powers in the adjacent delay bins to the Sinc function corresponding to a pulse width equal to the delay resolution. This essentially interpolates between the two bins to estimate the power and delay values for that peak. The taps are spaced with an interval of 3.33 ns starting from 0 ns with the first peak at $\tau = 1.94$ ns. There are also additional peaks corresponding to the remaining two specular peaks. The diffuse spectrum is modelled from the global PDP neglecting the power in the first three delay bins, noise level and the specular paths. The scaling factor α for different antenna polarisations is computed as the median of the difference between the estimated global PDP and polarisation-specific PDPs. Fig. 6 shows the global as well as polarization-specific PDPs, from which the values in (2) are taken. It should be noted that the proposed model is specific to the presently discussed relay antenna and measurement site.

TABLE I
DELAY AND POWER OF SPECULAR COMPONENTS

n	τ_n (ns)	P_n (dB)
1	1.94	-46.1
2	54.96	-62.5
3	201.67	-84.6

From Fig. 5, the direct coupling between the antenna ports on either side of the relay box is quite dominant as expected but there are significant multipath components arriving within 3.33 ns delay which would contain the reflections from the window and window frame. The other peaks occur at delays corresponding to approximately 16 m and 61 m propagation distance. From the layout shown in Fig. 3, it can be observed that the walls of the room on the side opposite to the antenna are at about 8 m distance from the antenna with the main beam pointing towards it. The peak at 16 m distance can be attributed to the first order reflection coming from the wall while the peak at 61 m distance can be attributed to the fourth order

reflection from the wall, i.e. reflected back and forth between the opposite wall and the antenna structure and windows four times. The peaks corresponding to the second and third order peaks are not visible as specular peaks as their power levels are within the diffuse component. Although the fourth order reflection at 61 m is about 40 dB lower than the largest component, due to the high isolation required for IBFD, it is necessary to model components such as this. From the PDP described in Eqn. (1), the number of taps required to model the SI channel can be calculated depending on the required SI cancellation level. If a system transmits 10 dBm power, a signal 90 dB below that corresponding to the specular path at 61 m propagation delay in Fig. 5 would have a signal strength of -80 dBm. This is still higher than the noise floor of a typical receiver and hence needs to be considered for the design of SI cancellation methods.

B. Fading characteristics of each tap

The fading characteristics of each significant tap are modelled by estimating the Rician K-factors. In this work, the significant taps refer to the ones with power 45 dB below the peak, so that the power is above the noise level of the measurement, leading to a model with 61 taps. The K-factor was calculated using the moment-based method [12]. CIRs from all measurement locations in the reception and coffee rooms respectively for different antenna heights are considered as fading realizations and are used to determine statistical models of the K-factors of each tap. The estimated K-factors are modelled as a normally distributed function with median μ and standard deviation σ which are enumerated in Table II. Fig. 7 shows the CDF of the K-factors for each tap, indicating that there is a dominant component visible in the first three taps, i.e., 0 ns, 3.33 ns and 6.66 ns. On visual observation, the K-factors of the remaining taps are more or less similar and hence, the K-factor from the fourth tap onwards is characterized by a single normally distributed probability density function. The median and standard deviation is computed from the observed K-factors of all the taps beyond the third tap.

IV. Conclusion

In this paper, a wideband SI channel model of compact back-to-back on-frequency repeater is presented. The repeater is meant for outdoor to indoor coverage extension. The model is based on a tapped delay line model with 300 MHz bandwidth centered at 2.6 GHz carrier frequency. The PDP is modelled as an exponentially decaying power spectrum with specular paths. The global PDP can extended to a polarization-specific PDP with the given scaling parameter. The fading characteristics of each tap are also modelled as normally distributed random variables. Depending on the target system bandwidth, the taps can be combined to reproduce wideband multipath SI channels for the design of SI cancellation methods.

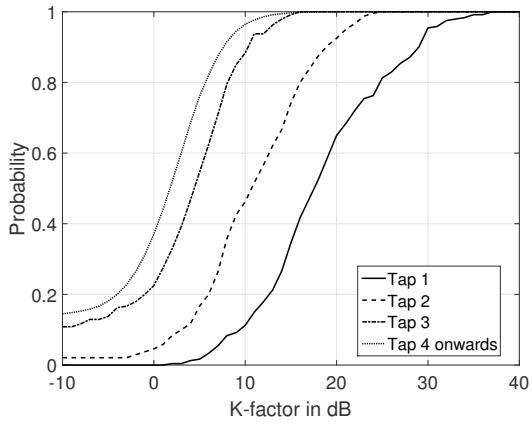

Fig. 7. Cumulative distribution function of the Rician K-factor for each tap. Modelled with normal distribution with parameters provided in Table II.

TABLE II
PARAMETERS OF THE NORMALLY DISTRIBUTED RICIAN K-FACTORS FOR DIFFERENT TAPS.

Tap no	τ (ns)	μ (dB)	σ (dB)
1	0	17.97	7.13
2	3.33	11.09	6.69
3	6.66	4.92	7.95
Tap 4 onwards	$\geq$10	2.25	7.5

References

[1] A. Sabharwal *et al.*, "In-band full-duplex wireless: Challenges and opportunities," *IEEE J. Sel. Areas Commun.*, vol. 32, no. 9, pp. 1637–1652, Sept 2014.

[2] M. Heino *et al.*, "Recent advances in antenna design and interference cancellation algorithms for in-band full duplex relays," *IEEE Commun. Mag.*, vol. 53, no. 5, pp. 91–101, May 2015.

[3] L. Laughlin, M. Beach, K. Morris, and J. Haine, "Optimum single antenna full duplex using hybrid junctions," *IEEE Journal on Selected Areas in Communications*, vol. 32, no. 9, pp. 1653–1661, Sept 2014.

[4] E. Everett *et al.*, "Passive self-interference suppression for full-duplex infrastructure nodes," *IEEE Trans. Wireless Commun.*, vol. 13, no. 2, pp. 680–694, February 2014.

[5] K. Haneda *et al.*, "Measurement of loop-back interference channels for outdoor-to-indoor full-duplex radio relays," in *Proc. of the 4th European Conference on Antennas and Propagation (EuCAP)*, 2010, pp. 1–5.

[6] S. Chen *et al.*, "Division-free duplex for wireless applications," *Electronics Letters*, vol. 34, no. 2, pp. 147–148, Jan 1998.

[7] T. Riihonen *et al.*, "SINR analysis of full-duplex OFDM repeaters," in *2009 IEEE 20th International Symposium on Personal, Indoor and Mobile Radio Communications*, 2009, pp. 3169–3173.

[8] A. Sahai *et al.*, "Pushing the limits of Full-duplex: Design and Real-time Implementation," Rice Uniersity, Houston, TX., Tech. Rep. TREE1104, 2011. [Online]. Available: http://arxiv.org/pdf/1107.0607.pdf

[9] L. Laughlin *et al.*, "A widely tunable full duplex transceiver combining electrical balance isolation and active analog cancellation," in *2015 IEEE 81st Vehicular Technology Conf. (VTC Spring)*, May 2015, pp. 1–5.

[10] T. Riihonen *et al.*, "Optimal eigenbeamforming for suppressing self-interference in full-duplex mimo relays," in *2011 45th Annual Conference on Information Sciences and Systems (CISS)*, March 2011, pp. 1–6.

[11] S. Venkatasubramanian *et al.*, "On the constrains to isolation improvement in multi-antenna systems," in *Eur. Conf. Antennas Propag.*, 2015, pp. 1–5.

[12] L. Greenstein *et al.*, "Moment-method estimation of the Ricean K-factor," *IEEE Commun. Lett.*, vol. 3, no. 6, pp. 175–176, June 1999.